J. Appl. Comput. Mech., 5(2) (2019) 217-230
DOI: 10.22055/JACM.2018.25429.1265

ISSN: 2383-4536
jacm.scu.ac.ir

M&MoCS

Shahid Chamran University of Ahvaz

Journal of Applied and Computational Mechanics

Research Paper

NURBS-Based Isogeometric Analysis Method Application to Mixed-Mode Computational Fracture Mechanics

Abdolghafour Khademalrasoul

Department of Civil Engineering, Faculty of Engineering, Shahid Chamran University of Ahvaz, Ahvaz, Iran

Received April 06 2018; Revised June 04 2018; Accepted for publication July 28 2018.
Corresponding author: A. Khademalrasoul, ag.khadem@scu.ac.ir

Abstract. An interaction integral method for evaluating mixed-mode stress intensity factors (SIFs) for two dimensional crack problems using NURBS-based isogeometric analysis method is investigated. The interaction integral method is based on the path independent J-integral. By introducing a known auxiliary field solution, the mixed-mode SIFs are calculated simultaneously. Among features of B-spline basis functions, the possibility of enhancing a B-spline basis with discontinuities by means of knot insertion makes isogeometric analysis method a suitable candidate for modelling discrete cracks. Moreover, the repetition of two different control points between two patches can create a discontinuity and also demonstrates a singularity in the stiffness matrix. In the case of a pre-defined interface, non-uniform rational B-splines are used to obtain an efficient discretization. Various numerical simulations for edge and center cracks demonstrate the suitability of the isogeometric analysis approach to fracture mechanics.

Keywords: NURBS; Isogeometric analysis method; Knot insertion; Interaction integral.

1. Introduction

The application of the isogeometric analysis approach is growing rapidly in various branches of engineering sciences. Fluid mechanics, solid mechanics, vibration analysis, soil and rock mechanics, and functionally graded materials (VALIZADEH, N. et al. (2013)) are some examples of isogeometric analysis applications. .

On the other hand, fracture mechanics and numerical methods have been considered over the few last decades in the mechanical engineering. Due to the appearance of defects in the structures, the fracture mechanics-based design is necessary to be taken into account. Therefore, the analysis of a cracked body is very crucial for engineers. In spite of the progress of mesh generators, the creation of the finite element mesh with a strong discontinuity remains extremely complicated. (Chen, T. et al. (2013); Daxini, S.D. and Prajapati, J.M. (2014); Zhuang, Z. et al. (2014)). On the other hand, a lot of errors in computational results may arise due to the approximation of the CAD (Computer Aided Design) in the finite element mesh. (Hughes, T.J.R. et al. (2009)). Because the advancements in engineering designs and construction technologies have been fast during latest years, the creation of the exact engineering geometries are very important. However, it has been demonstrated that the NURBS (Non-Uniform Rational B-splines) can create the exact geometry at least up to the second order surfaces. (Cottrell, J.A. et al. (2009); Hughes, T. J. R. et al. (2005)). In the isogeometric analysis method, the smooth geometric basis is used as the basis for both the analysis and the geometry approximation. Among various approaches for the computer aided design, NURBS are the most frequently adopted technologies in the isogeometric analysis framework. In fact, the smoothness of the basis functions plays a significant role in the accuracy of the engineering analysis. (Cottrell, J.A. et al. (2007); Cottrell, J.A. et al. (2006); Evans, J.A. et al. (2009)).

In reality, the isogeometric analysis approach uses the best capabilities of the meshless and the standard finite element methods. The IGA, unlike the conventional finite element method, the generation of the standard FE mesh, is alleviated. On the other hand, the control mesh improvement in the IGA is conducted using the knot insertion without changing the NURBS

Published online: January 19 2019

surfaces. Interface elements (Rots, J. (1991); Schellekens, J.C.J. and De Borst, R. (1993)) and embedded discontinuities (Oliver, J. (1996); Simo, J.C. et al. (1993)) are finite element technologies for capturing discontinuities. Nowadays, the partition of unity method (PUM or X-FEM, (Babuska, I., Melenk, J. (1997); Babuška, I. and Zhang, Z. (1998); Belytschko, T. and Black, T. (1999))) is considered as the most flexible element-based technology for capturing propagating cracks. One possibility of discretizing the cohesive zone formulation using isogeometric finite elements is to use them in combination with the partition of the unity method (De Luycker, E. et al. (2011); Ghorashi, S.S. et al. (2012)). In that case, the discontinuities would be embedded in the solution space by means of Heaviside functions. Moreover, the extended isogeometric analysis (XIGA) is utilized for cracked problems. In fact, the partition of unity concept is used in the XIGA. This technique also is used for buckling and vibration analysis (Bhardwaj, G. et al. (2015)), (Yin, S. et al. (2016))(Bui, T. Q. (2015)).

Although such an approach would be beneficial, but isogeometric finite elements offer the possibility to directly insert discontinuities in the solutions space. The conceptual idea is that in the isogeometric analysis approach, the inter element continuity can be decreased by means of knot insertion. In this study, however, we can create a strong discontinuity or a cohesive zone by using inherent specifications of NURBS basis functions. In addition to increasing the multiplicities of knot values in the parametric space, we can create a strong discontinuity in the physical domain with the repeated control points between two patches with identical coordinates. Moreover, the isogeometric analysis by using multi-patches domain is studied.

As a matter of fact, the possibility of continuity control in NURBS-based isogeometric analysis has become the IGA a capable approach in the fracture mechanics and also in the cohesive zone modelling. Since NURBS-based isogeometric analysis method possesses unique computational properties, therefore, it is possible to create different types of discontinuities by using these facilities. Hence, this analysis method may be attractive for engineers. On the other hand, the isogeometric analysis method can create the discontinuities by using its mathematical abilities. However, these inherent properties of the isogeometric analysis led us to use this method in the computational fracture mechanics.

The remainders of this study are as follows. First, in the rest of Section 1, the main topics on isogeometric analysis and NURBS are discussed. The principles of fracture mechanics are explained in Section 2. Section 3 introduces the major concepts of discontinuity creating in B-splines basis functions and also introduces the discretization concept in the isogeometric analysis method. Furthermore, the numerical simulations for 2D problems are studied in Section 4. Finally, conclusions are summarized in Section 5.

1.1. NURBS

In general, B-splines are piecewise polynomials that offer great flexibility and precision for a myriad of modeling applications. They are built from a linear combination of basis functions. (Bazilevs, Y. et al. (2010); Hughes, T.J.R. et al. (2005); Scott, M.A. et al. (2012)). These basis functions are locally supported and have continuity properties that follow directly from those of the basis (Hughes, T.J.R. et al. (2005)). However, there are geometric entities in $\mathbb{R}^{d_s}$ that cannot be modeled exactly by piecewise polynomials. Many important ones, however, can be obtained through a projective transformation of a corresponding B-spline entity in $\mathbb{R}^{d_s+1}$ yielding a rational B-spline. In particular, conic sections, such as circles and ellipses, can be exactly constructed by projective transformations of piecewise quadratic curves (Hughes, T.J.R. et al. (2009); Piegl, L.A. and Tiller, W. (1997); Rogers, D. F. (2001)).

NURBS curve is a parametric curve, meaning that the points on the curve are swept out as the curve's parameter changes (Mathematically, the parameters of a curve or surface are the independent variables in the expression for the curve/surface). NURBS-based isogeometric analysis method can preserve the exact geometry, convenient for the free-form surface modeling and also possesses special mathematical properties. NURNS basis functions can be refined through knot insertion; in fact each NURBS of order p is C^{p-1}- continuous. In addition, the convex hall and variation diminishing properties are other NURBS mathematical specifications (Hughes, T.J.R. et al. (2009); Piegl, L.A. and Tiller, W. (1997)). Consequently, these NURBS' merits properties have changed it to be interesting for the fracture mechanics. A NURBS surface and solid are defined as follows:

$$\mathbf{S}(\boldsymbol{\xi}) = \sum_{\mathbf{i}\in I} \mathbf{P}_{\mathbf{i}}\, R_{\mathbf{i},\mathbf{p}}(\boldsymbol{\xi}), \tag{1}$$

where $\mathbf{P}_i$ is a set of control points, $R_{\mathbf{i},\mathbf{p}}$ is multivariate basis function, and ξ is a parameter value. A multivariate basis function is defined according to the univariate counterpart. Univariate B-spline basis functions for a given order p are defined recursively in the parametric space by way of the knot vector $\Xi = \{\xi_1, \xi_2, \xi_3, \ldots, \xi_{n+p+1}\}$, where n is the number of basis functions which comprise the B-spline and are in a one to one correspondence with the control points and also are not in a one to one correspondence with the knots. A knot vector is a non-decreasing sequence of coordinates in the parametric space (COX, M.G. (1972); de Boor, C. (1972)). The length of a knot vector is considered to $n+p+1$. The corresponding multivariate NURBS basis function is defined as (Bazilevs, Y. et al. (2010))

$$R_{\mathbf{i},\mathbf{p}}(\xi) = \frac{w_{\mathbf{i}}\, B_{\mathbf{i},\mathbf{p}}(\xi)}{\sum_{\mathbf{j}\in I} w_{\mathbf{j}}\, B_{\mathbf{j},\mathbf{p}}(\xi)}, \tag{2}$$

where $\{w_{\mathbf{i}}\}_{\mathbf{i}\in I}$ is a set of weights and I is the appropriate index set. A multivariate NURBS basis functions are defined using subsequent relation,

$$B_{\mathbf{i},\mathbf{p}}(\xi)=\prod_{l=1}^{d_p} N^{l}_{il,pl}\left(\xi^{l}\right), \tag{3}$$

where $d_p = 1, 2, 3, \ldots$ is corresponding to the dimension of the problem and l must not confused with the power, therefore, this superscript implies any direction in the domain. Multivariate NURBS basis functions inherit most of the properties of their univariate counterparts, namely partition of unity, nonnegativity, compact support, higher-order continuity, and linear independence (Bazilevs, Y. et al. (2010); Bazilevs, Y. et al. (2012)). Univariate B-spline basis functions $N_{i,p}$ is defined recursively using Cox-de-Boor formula as follows(COX, M.G. (1972; de Boor, C. (1972)):

First, beginning with piecewise constant ($p = 0$), then we have

$$N_{i,0}=\begin{cases}1 & \text{if} \quad \xi_i \le \xi < \xi_{i+1},\\ 0 & \text{Otherwise.}\end{cases} \tag{4}$$

Therefore, for $p = 1,2,3,\ldots$, the basis functions according to the aforementioned formula is defined in the following way:

$$N_{i,p}=\frac{\xi-\xi_i}{\xi_{i+p}-\xi_i}N_{i,p-1}(\xi)+\frac{\xi_{i+p+1}-\xi}{\xi_{i+p+1}-\xi_{i+1}}N_{i+1,p-1}(\xi). \tag{5}$$

Figure 1 shows a NURBS surface and also some control points which do not coincide the surface.

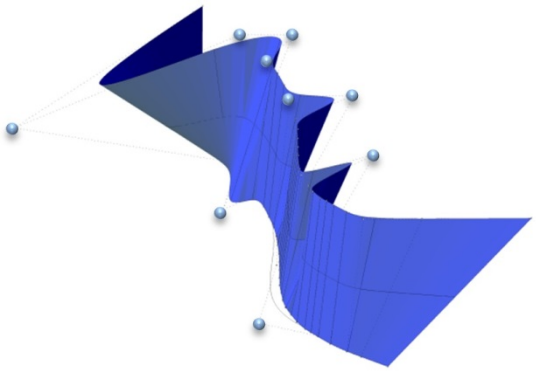

Fig. 1. The NURBS Surface with its Associated Control Points.

2. Principles of fracture mechanics

The stress intensity approach is utilized to characterize the behavior of a body with a discontinuity such as crack and flaw, in linear elastic fracture mechanics. Besides, during last decades, much effort has been done on SIFs calculations (Bandyopadhyay, S.N. and Deysarker, H.K. (1981); Joseph, R.P. et al. (2014; Kim, H.-K. and Lee, Y.-H. (2014); Kim, J.-H. and Paulino, G.H. (2003); Likeb, A. et al. (2014); Sutradhar, A. and Paulino, G.H. (2004); Tur, M. et al. (2006)). Theoretical, numerical, and experimental methods have been employed for determination of the SIFs in the vicinity of crack tips in the cracked bodies. There are three basic modes of deformation according to three independent kinematic movements of upper and lower crack surfaces with respect to each other. Any deformation of crack surfaces can be viewed as a superposition of these basic deformation modes, which are as opening, sliding, and tearing (antiplane) modes. In 2D numerical analysis, we only calculate the two first modes of deformations and so the corresponding stress intensity factors.

For two dimensional and any linear elastic body, the crack-tip stress fields is given by a series of the form Eq.(6) which is known as Williams' asymptotic solution (Williams, M.L. (1957)) as follows:

$$\sigma_{ij}(r,\theta)=A_1 r^{-1/2} f_{ij}^{(1)}(\theta)+A_2 f_{ij}^{(\theta)}+A_3 r^{1/2} f_{ij}^{(3)}(\theta)+\text{higher order terms}, \tag{6}$$

where σ_{ij} is the stress tensor, r and θ are polar coordinates with the origin at the crack-tip. Moreover, $f_{ij}^{(1)}$, $f_{ij}^{(2)}$, $f_{ij}^{(3)}$ are universal functions of θ, and A_1, A_2, A_3 are parameters proportional to the remotely applied loads. In the vicinity of the crack tip, where ($r \to 0$), the leading term which has the denominator of square-root exhibits singularity. The amplitude of the singular stress fields is characterized by the stress intensity factors (SIFs), i.e., (Gdoutos, E.E. (2005); Mohammadi, S. (2008))

$$\sigma_{ij}=\frac{K_{\mathrm{I}}}{\sqrt{2\pi r}}f_{ij}^{(1)}(\theta)+\frac{K_{\mathrm{II}}}{\sqrt{2\pi r}}f_{ij}^{(2)}(\theta)+\frac{K_{\mathrm{III}}}{\sqrt{2\pi r}}\mathrm{f}_{ij}^{(3)}, \tag{7}$$

where $K_{\mathrm{I}}, K_{\mathrm{II}}$, and K_{III} are the mode I, II, and mode III of the SIFs, respectively. By assuming the small-scale yielding in an elastic body, we can assume the crack as a semi-infinite domain. Therefore, by ignoring the higher order terms in the series, the first order equations of the stress fields for mode I are as follows (Gdoutos, E.E. (2005)):

$$\begin{bmatrix}\sigma_{xx}\\ \sigma_{yy}\\ \tau_{xy}\end{bmatrix}=\frac{K_{\mathrm{I}}}{\sqrt{2\pi r}}\cos\frac{\theta}{2}\begin{bmatrix}1-\sin\frac{\theta}{2}\sin\frac{3\theta}{2}\\ 1+\sin\frac{\theta}{2}\sin\frac{3\theta}{2}\\ \sin\frac{\theta}{2}\cos\frac{3\theta}{2}\end{bmatrix} \tag{8}$$

2.1. Interaction integral (M-integral)

The interaction integral is derived from the path-independent *J*-integral for two admissible states of a cracked elastic body. *J*-integral as a path independent integral, originally introduced by J.R. Rice to evaluate strain concentration by notches and cracks in a linear elastic or non-linear elastic and deformation-type elastic-plastic materials (Rice, J.R. (1968)). The *J*-integral is based on an energy balance and is equivalent to the energy release rate during crack extension in a homogeneous elastic body (de Klerk, A. et al. (2008)).The *M*-integral is the dual form of the *J*-integral. The *M*-integral is based on the principle of complementary energy (de Klerk, A. et al. (2008)). In fact, by utilizing the interaction integral, the two first values of the stress intensity factors (i.e., K_{I} and K_{II}) could be calculated in one step. Furthermore, the computational efforts may decrease.

Consider a 2-D homogeneous crack body of linear or non-linear material free of body forces and tractions on the crack surfaces; the *J*-integral in numerical methods is usually defined as:

$$J=\lim_{\Gamma\to 0}\int_{\Gamma}(W\,\delta_{1j}-\sigma_{ij}u_{i,1})n_j\ \mathrm{d}\Gamma, \tag{9}$$

where W is the strain energy density given by:

$$W=\int_0^{\varepsilon_{kl}}\sigma_{ij}\,d\,\varepsilon_{ij} \tag{10}$$

and n_j denotes the outward normal vector to the contour Γ, as shown in Fig. 2.

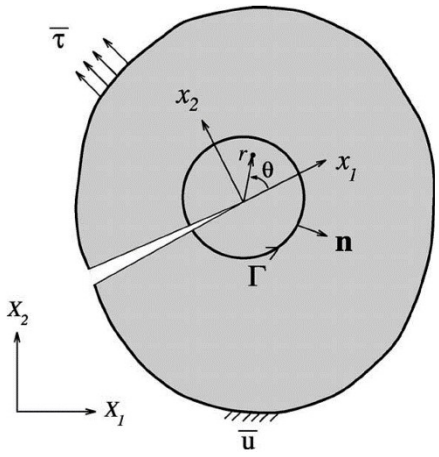

Fig. 2. General representation of a cracked body, polar coordinate (r,θ) with the origin at the crack tip and *J*-integral path (Γ).

State 1 ($\sigma_{ij}^{(1)}$, $\varepsilon_{ij}^{(1)}$, $u_i^{(1)}$) corresponds to the actual state and state 2 ($\sigma_{ij}^{(2)}$, $\varepsilon_{ij}^{(2)}$, $u_i^{(2)}$) is an auxiliary state which is chosen as the asymptotic fields for modes I and II. The *J*-integral for the sum of the two states is as follows:

$$J^{(1+2)}=\int_{\Gamma}\left[\frac{1}{2}(\sigma_{ij}^{(1)}+\sigma_{ij}^{(2)})(\varepsilon_{ij}^{(1)}+\varepsilon_{ij}^{(2)})\,\delta_{1j}-(\sigma_{ij}^{(1)}+\sigma_{ij}^{(2)})\frac{\partial(u_i^{(1)}+u_i^{(2)})}{\partial x_1}\right]n_j\,d\,\Gamma \tag{11}$$

Expanding and rearranging terms gives:

$$J^{(1+2)}=J^{(1)}+J^{(2)}+M^{(1,2)} \tag{12}$$

where $M^{(1,2)}$ is called the interaction integral for states 1 and 2

$$M^{(1,2)}=\int_{\Gamma}\left[W^{(1,2)}\delta_{1j}-\sigma_{ij}^{(1)}\frac{\partial u_i^{2}}{\partial x_1}-\sigma_{ij}^{(2)}\frac{\partial u_i^{1}}{\partial x_1}\right]n_j\,d\,\Gamma \tag{13}$$

and $W^{(1,2)}$ is the interaction strain energy density as follows:

$$W^{(1,2)}=\sigma_{ij}^{(1)}\,\varepsilon_{ij}^{(2)}=\sigma_{ij}^{(2)}\,\varepsilon_{ij}^{(1)} \tag{14}$$

Then according to the relationship between the values of *J*-integral and the stress intensity factors for the combined states

after rearranging terms we have:

$$J^{(1+2)} = J^{(1)} + J^{(2)} + \frac{2}{E_{\text{eff}}}(K_{\text{I}}^{(1)} K_{\text{I}}^{(2)} + K_{\text{II}}^{(1)} K_{\text{II}}^{(2)}) \tag{15}$$

Therefore, we can write

$$M^{(1,2)} = \frac{2}{E_{\text{eff}}}(K_{\text{I}}^{(1)} K_{\text{I}}^{(2)} + K_{\text{II}}^{(1)} K_{\text{II}}^{(2)}) \tag{16}$$

where E_{eff} is defined in terms of material parameters E (Young's modulus) and ν (Poisson's ratio) as follows:

$$E_{\text{eff}} = \begin{cases} E, & \text{Plane Stress} \\ \dfrac{E}{1-\nu^2}, & \text{Plane Strain} \end{cases} \tag{17}$$

Finally, the stress intensity factors for the current state can be found by separating the two modes of fracture in 2-D problems. Moreover, the contour integral defining $M^{(1,2)}$ is converted into an area integral by multiplying the integrand by a bounded smoothing function $q(x)$; that is 1 on an open set containing the crack tip and vanishes on an outer prescribed contour Γ_0. Then for each contour Γ (as shown in Fig. 3) in this open set where $q(x)=1$ and assuming the crack faces are stress free and straight in the interior of the region A bounded by the prescribed contour Γ_0, the interaction integral may be written as:

$$M^{(1,2)} = \int_C \left[W^{(1,2)} \delta_{1j} - \sigma_{ij}^{(1)} \frac{\partial u_i^{(2)}}{\partial x_1} - \sigma_{ij}^{(2)} \frac{\partial u_i^{(1)}}{\partial x_1} \right] q\, m_j \, d\Gamma \tag{18}$$

where $C = \Gamma + C_+ + C_- + \Gamma_0$ and $\mathbf{m}$ is the outward unit normal to the contour C. Moreover, due to simplification of the numerical calculations, the *M*-integral is formulated on an equivalent domain area of integration as follows:

$$M^{(1,2)} = \int_A \left[\sigma_{ij}^{(1)} \frac{\partial u_i^{(2)}}{\partial x_1} + \sigma_{ij}^{(2)} \frac{\partial u_i^{(1)}}{\partial x_1} - W^{(1,2)} \delta_{1j} \right] \frac{\partial q}{\partial x_j} \, dA \tag{19}$$

The condition that the smoothing function is 1 on an open set containing the crack tip is easily relaxed to be just equal 1 at the tip. The interaction integral is calculated using stresses and strains of the Gaussian integration points in the isogeometric analysis framework. Figure 4 demonstrates the implementation of *M*-integral in the isogeometric analysis framework using the index space.

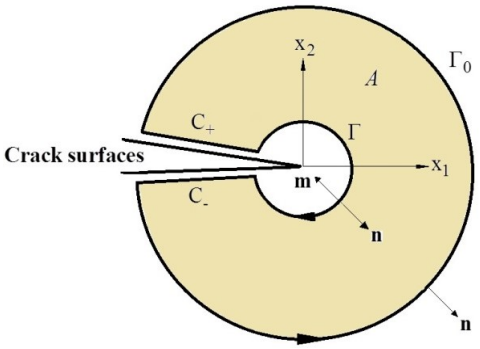

Fig. 3. Illustration of the equivalent domain area for implementing M-integral.

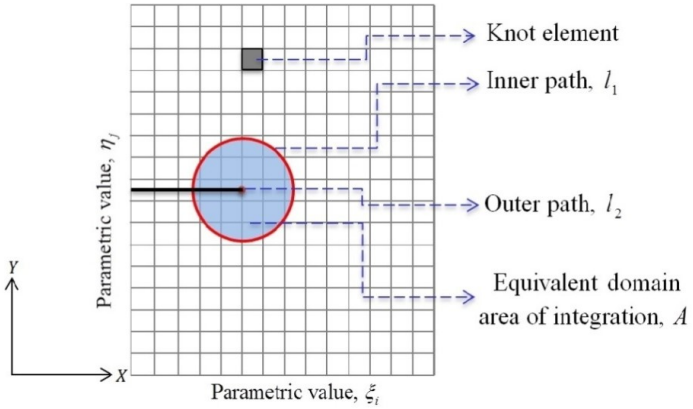

Fig. 4. Implementation of M-integral in the parametric space.

3. Discontinuities in B-splines, NURBS

The fundamental building block of the isogeometric analysis is the univariate B-spline (Hughes, T.J.R. et al. (2009); Piegl, L. and Tiller, W. (1997); Rogers, D.F. (2001)). A univariate B-spline is a piecewise polynomial defined over a knot vector $\Xi = \{\xi_1, \xi_2, \xi_3, \ldots, \xi_{n+p+1}\}$, where n is the number of basis functions and p is the polynomial order. As a consequence, the knots divide the parametric domain $[\xi_1, \xi_{n+p+1}] \subset \mathbb{R}$ in knot intervals of non-negative length. We refer to knot intervals of positive length as elements, therefore, we have the knot elements. When several knot values coincide, their multiplicity is indicated by m_i, where i corresponds to the index of the knot values. The B-splines used for analysis purposes are generally open B-splines, which means that the multiplicity of the first and last knots (i.e., m_1 and m_{n+p+1}) are equal to $p+1$. The property of NURBS of particular interest for the fracture mechanics is that they are $p-m_i$ times continuously differentiable over a knot i. This allows for the direct discretization of higher-order differential equations (Gómez, H. et al. (2008)). The ability to control the inter-element continuity is useful for cohesive zone models since discontinuities can be inserted arbitrarily by means of knot insertion. In fact, a jump in the displacement field at a certain point $x_d = x(\xi_d)$ in the physical space can be created by raising the multiplicity of the knot ξ_d to $m_i = p+1$.

Furthermore, it is possible to create the strong discontinuity in the isogeometric analysis framework by utilizing the repetition of two different coincided control points between two patches. As a consequence, the singularity is happened in the stiffness matrix and then the influences of crack areimposed on the cracked plate. Figure 5 schematically depicts the procedure of crack modeling in the IGA approach.

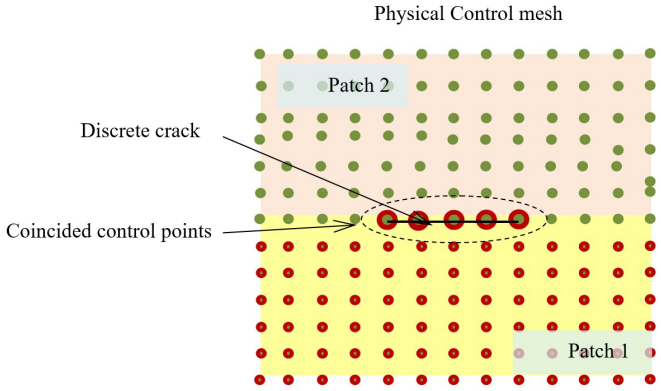

Fig. 5. Discretization scheme for crack modeling in the IGA method

3.1. Discretization of solids using NURBS

In this section, the formulation of two dimensional problems is discussed. NURBS (or B-spline), basis functions are used for both the parameterization of the geometry and the approximation of the solution space for the displacement field $\mathbf{u}$ that is,

$$\mathbf{u}(\xi,\eta) = \sum_{i=1}^{n}\sum_{j=1}^{m} R_{i,j}^{p,q}(\xi,\eta)\mathbf{U}_{i,j}, \tag{20}$$

where $R_{i,j}^{p,q}$ are the bivariate NURBS basis functions and $\mathbf{U}_{i,j}$ are the displacement control variables. The parameterization of a body $\Omega \subset \mathbb{R}^2$ can be obtained by a NURBS surface. Such a surface can be comprised of one or more NURBS surfaces. A two-dimensional NURBS patch (i.e., any B-spline associated with a particular set of knot vectors, polynomial orders, and control points is referred as a patch.) gives a bivariate parameterization of Ω based on the knot vectors $\Xi = \{\xi_1, \xi_2, \xi_3, \ldots, \xi_{n+p+1}\}$, and, $\mathcal{H} = \{\eta_1, \eta_2, \eta_3, \ldots, \eta_{m+q+1}\}$, such that $(\xi, \eta) \in [\xi_1, \xi_{n+p+1}] \otimes [\eta_1, \eta_{m+q+1}] \subset \mathbb{R}^2$.

$$\mathbf{x}(\xi,\eta) = \sum_{i=1}^{n}\sum_{j=1}^{m} R_{i,j}^{p,q}(\xi,\eta)\mathbf{X}_{i,j}, \tag{21}$$

where $\mathbf{X}_{i,j}$ are the coordinates of the control points. It should be noted that when all weights of control points are equal and in the especial form equal to one, therefore, NURBS basis functions degenerate to B-spline counterparts.

4. Numerical Example

In this section, NURBS surfaces with predefined strong discontinuity such as edge and center cracks are considered. First of all, for each plate which assumed under uniaxial tension, the comparison between the exact solution and the isogeometric analysis results are performed to show the accuracy of the numerical solutions. All NURBS surfaces are created with

polynomial order 3 in both geometrical directions. The stress distribution condition is assumed as the plane strain and the material constitutive is considered as linear elastic. Eventually, the values of the stress intensity factors are numerically calculated and also compared with the analytical-experimental counterparts. On the other hand, in order to represent the condition of the stiffness matrix, the eigenvalues for each model are calculated and the largest to smallest eigenvalues' ratio ($\lambda_{max}/\lambda_{min}$) is obtained. The maximum to minimum ratio of eigenvalues is named "stiff index". In reality, a matrix is called *stiff* if the ratio is much greater than one.

4.1. Finite plate with an single edge crack (SEC)

In the first example, a predefined edge crack with the length of 0.5 in a 3×6 plate under uniaxial tension is modeled. This model is discretizes using different pattern of control nets. We utilized two models which comprised of 1233 and 3336 number of control points. As a matter of fact, the arrangement of control points is considered in a manner to have the maximum control on the NURBS surface in the vicinity of the crack tip. Therefore, we have the topologically rectangular finer control net around the crack tip. In addition, to increase the precision of the numerical integration we have used the finer parametric space in the vicinity of the crack tip. Therefore, we have the finer knot spans around the crack tip. Moreover, due to capturing the sudden changes in stresses at the crack tip, the polynomial order of 3 are implemented in all geometrical directions. All models are constructed with two patches, and every patch contains 625 (25×25) and 1683 (51×33) individual control points. Hereupon, the length of each knot vector which is associated with its corresponding geometrical direction considered as $p+n+1$ and $q+m+1$.Therefore, in the first model, we choose the knot vector in x and y directions with the length of 29 and in the second model, the length of the knot vector in x direction is 55 and in y direction is 37. Besides, since all knot vectors are open, therefore, the first and last knot values multiplicities are 4. The constitutive of material is assumed as linear elastic with the properties of $E=1.0\text{E+06}\,(\text{MPa})$ and $\nu=0.3$. Figure 6 illustrates the stress distribution and stress concentration at the crack tip and depicts the smooth sudden changes that occur in the plate with an edge crack. What is so crucial in computational fracture mechanics using the isogeometric analysis is the smoothness of stress distribution throughout the body, particularly in the vicinity of the crack tip. It should be noted that, the precision of stress and strain at the crack tip are very important since they are used to calculate the stress intensity factors and the initiation angle of crack growth. Unlike other numerical approaches, the inter-element degrees of continuity are easily obtained in the isogeometric analysis framework.

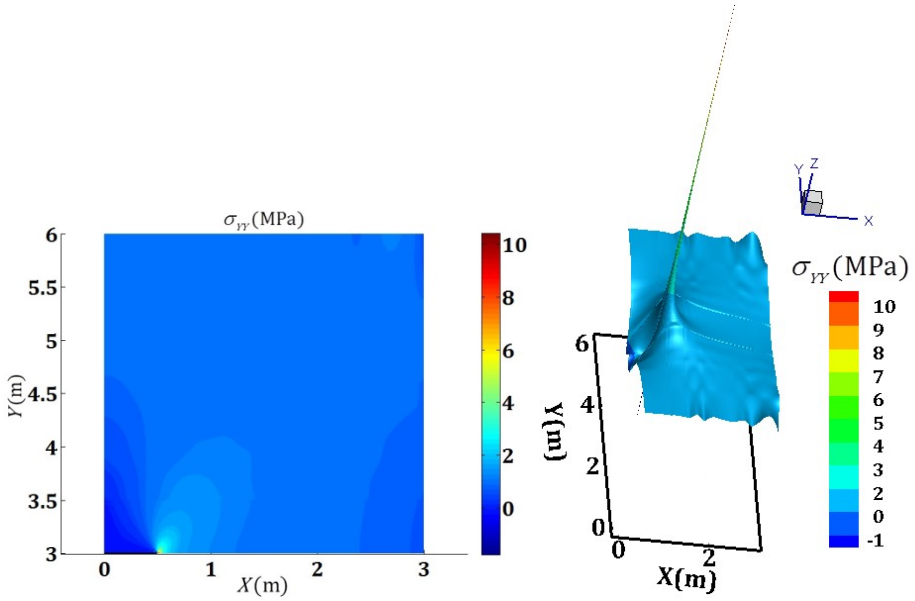

Fig. 6. Distribution of σ_{yy} in a plate with an edge crack.

Figure 7 shows the comparison between the exact solutions for the plate with an edge crack with the length of 0.5. In this example, the adjacent of IGA solution with the approximation polynomial order of 3, the finer control grid around the crack tip, and also the finer parametric space around the crack tip are guaranteed the precise results. As it is clear, by using more control points, particularly around the crack tip, the accuracy of the results increases. Therefore, we represent the results of the second model with more degrees of freedom.

In order to demonstrate the smoothness of stress distribution in front of the crack tip, we calculate the values of the SIFs via stress extrapolation approach as well. According to the stress extrapolation approach, the magnitude of the mode I and II stress intensity factors (K_{I} and K_{II}) for aforementioned plate under uniaxial tension are obtained and summarized in details in Table 1. As it shown in Table 1, the stiff index decreases with the increasing of the degrees of freedom (DOFs). In fact, the excess DOFs which are considered around the crack tip would be beneficial to evaluate better the stress singularity at the crack tip and consequently are important to change the stiffness matrix to a well-conditioned.

The values of the experimental-analytical solutions for edge crack problems are calculated using Eq. (22):

$$K_I = \left[1.12 - 0.23\left(\frac{a}{b}\right) + 10.56\left(\frac{a}{b}\right)^2 - 21.74\left(\frac{a}{b}\right)^3 + 30.42\left(\frac{a}{b}\right)^4\right]\sigma\sqrt{\pi a}, \tag{22}$$

where a is the length of the crack, b is the width of the considered plate, and σ is the applied remote stress.

Table 1. Values of the stress intensity factors based on stress extrapolation approach for SEC model.

Crack length	Analytical-Experimental K_I	Number of control points	K_I	K_{II}	K_I/K_I (Analytical)	Stiff index
0.5	1.6266	1233	1.6850	0.001	1.036	1.56
0.5	1.6266	3336	1.6360	0.003	1.005	1.17

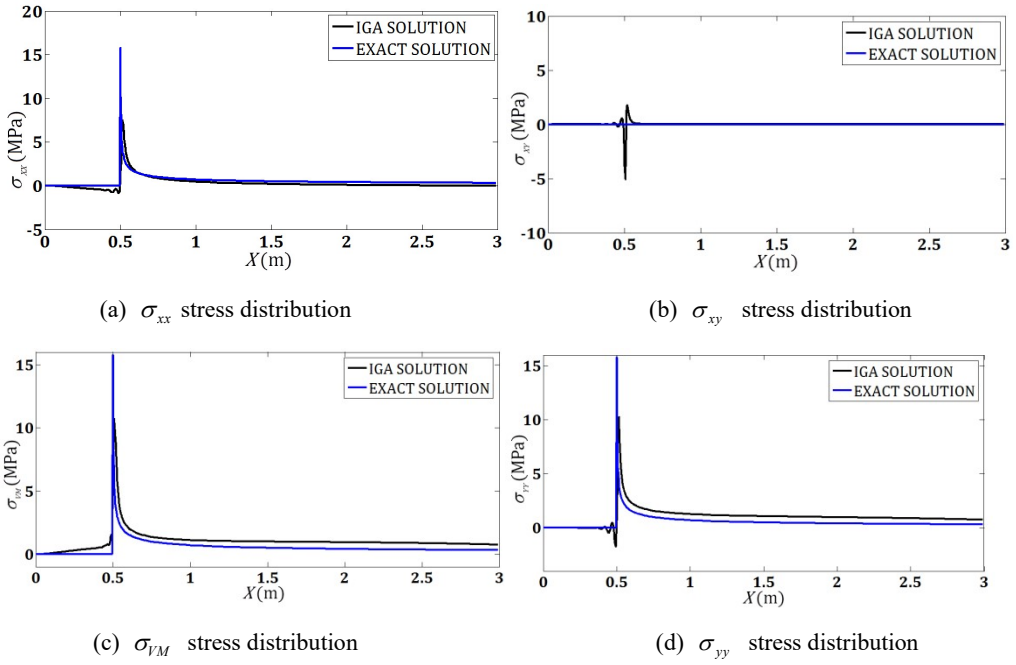

Fig. 7. The comparison between the exact solutions and IGA results for edge crack problem.

In this study, we attempt to demonstrate the possibility of isogeometric analysis method in calculating of the fracture mechanic parameters. Therefore, the values of computational stress intensity factors for mode I and II are compared with the analytical-experimental counterparts. Moreover, in the plane strain condition and for a plate with the width of 3 and the height of 6, the values of SIFs are calculated using the interaction integral method which is known as *M*-integral.

In this comparison, the length of each kind of the crack is chosen variable. In fact, according to the geometry restrictions, the lengths of the crack are chosen from 0.1 to 2.0.Table 2 and Fig. 8 illustrate the compatibility of the computational and the analytical SIFs which are calculated for a plate with an edge crack. Because the width of the domain is 3, therefore, when the edge crack length is 2.0, and as it approaches to the boundary of the domain, we have the maximum error in SIFs. As we can see in Table 2, the values of the SIFs which are numerically calculated using *M*-integral are close to the analytical-experimental counterparts.

Table 2. Comparison between analytical-experimental values of stress intensity factors and numerical results for edge crack problems

Crack length	Analytical-Experimental K_I	Numerical K_I	Numerical K_{II}	K_I(Numerical)/K_I(Analytical)
0.1	0.6296	0.6251	0.0018	0.993
0.2	0.9082	0.9135	0.0025	1.006
0.3	1.1493	1.1547	0.0032	1.005
0.4	1.3846	1.3869	0.0038	1.001
0.5	1.6266	1.6258	0.0044	0.999
0.6	1.8825	1.8789	0.0051	0.998
0.7	2.1581	2.1535	0.0058	0.998
0.8	2.4591	2.4532	0.0008	0.998
0.9	2.7927	2.7905	0.0009	0.999
1.0	3.1674	3.1708	0.001	1.001
1.5	6.1407	6.1340	0.0161	0.999
2.0	13.1032	13.4695	0.0038	1.028

4.2. Finite plate with a horizontal center crack (CC)

In the following example, a predefined horizontal center crack with the length of 0.5 in a 3×6 plate under uniaxial tension is modeled. In order to visualize the effects of the control point's pattern, this plate is discretized by using of the three different patterns of the physical control points. We establish the models with 1230, 4010, and 9876 physical control points. As a matter

of fact, the arrangement of control points is considered in a manner to have the maximum control on the NURBS surface in the vicinity of the crack tips. The finer discretization not only is obtained by using finer physical control mesh but also in the parametric space. However, more DOFs improve the stiffness matrix condition. Moreover, due to capturing the sudden changes in the stresses at the crack tips, the polynomial order 3 are utilized in all geometrical directions. These examples are constructed with two patches and every patch comprises of625 (25×25), 2025 (45×45), and 4978 (131×38) individual control points, respectively. Besides, the lengths of the knot vector for every model are become (29×29), (49×49) and (135×42), respectively.

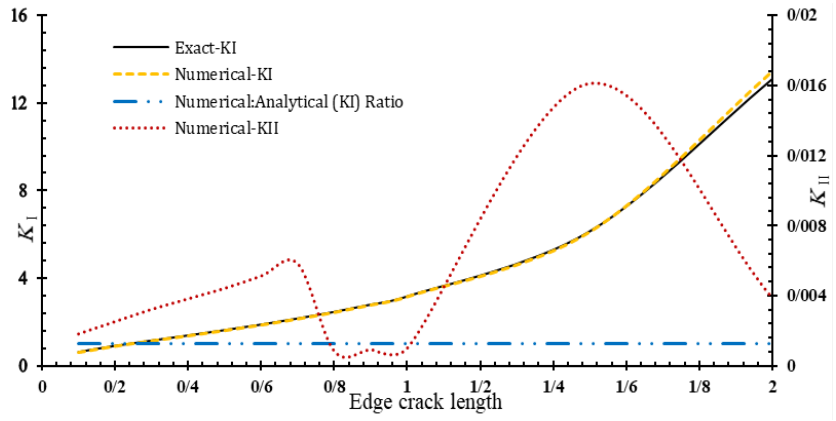

Fig. 8. Representation of the numerical and theoretical calculations of the SIFs for edge crack problems**.**

The constitutive of material for stress distribution condition is the plane strain and the properties of elasticity are assumed as $E = 1.0\,\mathrm{E}+06(\mathrm{MPa})$ and $\nu = 0.3$. Figure 9 illustrates the stress distribution and stress concentration at the crack tips and also the sudden changes that occurs in the plate.

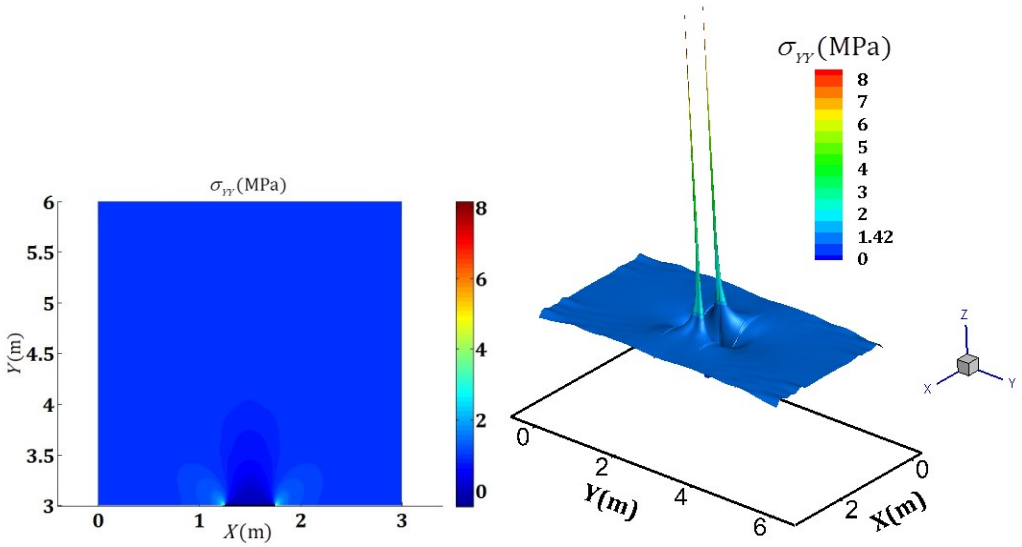

Fig. 9. Isogeometric analysis result of σ_{yy} distribution for center crack example.

Then, in order to demonstrate the smoothness of the stress distribution throughout the plate, we extract the obtained results at the level of the crack tips (i.e., y = 3) and finally compare them with the exact solutions. The numerical results represent a significant adaptation with the exact counterpart amounts. In fact, utilizing polynomial order three preserve the smoothness and precision of the stresses and strains. The results are depicted in Fig. 10.

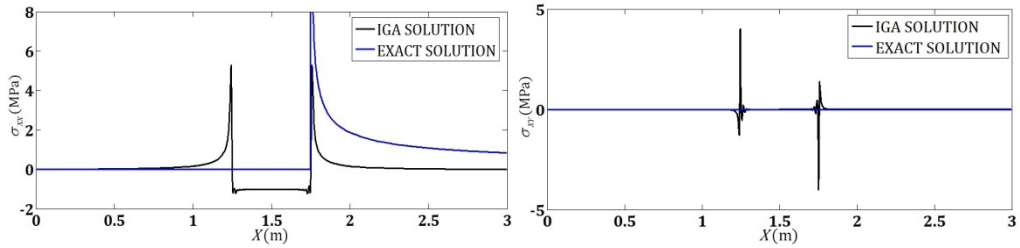

(a) σ_{xx} stress distribution (b) σ_{xy} stress distribution

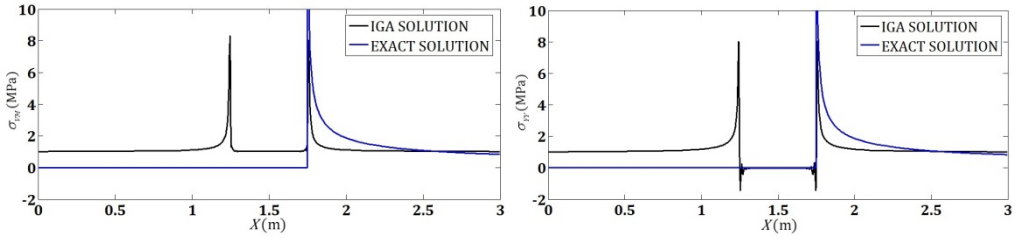

(c) σ_{VM} stress distribution (d) σ_{yy} stress distribution

Fig. 10. Comparison between the exact solutions and IGA results for center crack problem.

As it is known, one of the most important issues in the context of the numerical approaches is the stiffness matrix. However, in this example with three different discretization schemes and degrees of freedom (DOFs), we have three stiffness matrices with their particular own properties. Among various properties of the stiffness matrix, we restrict ourselves to the "*stiff index*" which is defined as the largest to smallest ratio of the corresponding eigenvalues.

However, we calculate the values of the SIFs via the stress extrapolation approach as well. According to the stress extrapolation approach, the magnitude of the mode I and II stress intensity factors (i.e., K_{I} and K_{II}) for aforementioned plates under uniaxial tension are obtained and summarized in details in Table 3. As it is shown in Table 3, the *stiff index* decreases with the increasing of the degrees of freedom (DOFs). In fact, the excess DOFs which are considered around the crack tips would be beneficial to evaluate better the stress singularity at the crack tip and consequently would be important to change the stiffness matrix to a well-conditioned.

The values of the experimental-analytical solutions for center crack problems are calculated using Eq. (23):

$$K_{\mathrm{I}} = \left[1+0.256\left(\frac{a}{b}\right)-1.152\left(\frac{a}{b}\right)^{2}+12.2\left(\frac{a}{b}\right)^{3}\right]\sigma\sqrt{\pi a} \tag{23}$$

Table 3. Values of the stress intensity factors based on stress extrapolation approach for CC model.

Crack length	Analytical-Experimental K_{I}	Number of control points	K_{I}	K_{II}	$K_{\mathrm{I}}/K_{\mathrm{I}}$ (Analytical)	Stiff index
0.5	0.9043	1230	0.9103	0.056	1.006	1.850
0.5	0.9043	4010	0.8970	0.011	0.992	1.690
0.5	0.9043	9876	0.9033	0.011	0.999	1.003

In order to calculate the mixed mode stress intensity factors, the *M*-integral is implemented in the IGA framework. Therefore, we are able to obtain the mixed mode SIFs at one step. In fact, using interaction integral decreases the computational efforts in the numerical context rather than using *J*-integral for mixed mode problems. Moreover, the horizontal center cracks with different lengths are modeled to examine the capability of the IGA method in the fracture mechanics. In fact, having the precise mixed mode stress intensity factors helps us understand the accurate crack initiation angle of growth. All present examples are under uniaxial tension loading. According to the geometry configuration and loading conditions, we obtained the symmetric results for both crack tips in the domain. The results are listed in Table 4. As it is shown, the error slightly increases in estimating the SIFs as the length of the center crack increases. While the crack tips are approaching to the edges of the domain (i.e., geometrical boundaries), the error increases.

Furthermore, Fig. 11 illustrates the compatibility of the numerical and analytical-experimental values of SIFs for center crack problems.

Table 4. Comparison between analytical-experimental values of stress intensity factors and numerical results for center crack problems

Crack length	Analytical-Experimental K_{I}	Numerical K_{I}	Numerical K_{II}	K_{I}(Numerical)/K_{I} (Analytical)
0.1	0.3979	0.3982	0.0000	1.001
0.2	0.5648	0.5434	0.0000	1.01
0.3	0.6943	0.6787	0.0000	0.976
0.4	0.8050	0.7919	0.0000	0.984
0.5	0.9043	0.8988	0.0000	0.994
0.6	0.9963	0.9810	0.0000	0.985
0.7	1.0838	1.0701	0.0000	0.987
0.8	1.1687	1.1566	0.0000	0.990
0.9	1.2528	1.2422	0.0000	0.992
1.0	1.3375	1.3278	0.0000	0.993
1.5	1.8153	1.7940	0.0000	0.988
2.0	2.4977	2.4517	0.0000	0.982

4.3. Slanted center crack in a finite plate

In this section, four different slanted center cracks with different angles are modeled. There are15, 30, 45, and 60 degrees oriented center cracks studied to demonstrate the capabilities of the isogeometric analysis method in strong crack creation and SIFs calculation. In fact, we are encountered with the mixed mode condition in those considered models. Therefore, we have to calculate the two first values of the stress intensity factors (i.e., K_{I} and K_{II}).

Consider a plate containing a single interior crack of length $2a$ oriented at an angle θ with the horizontal direction as shown in Fig. 12, where λ is the lateral load ratio. The analytical values of the SIFs for oriented center cracks are obtained using Eq. (24). When the uniaxial loading is considered then $\lambda = 0$. Then, for a uniaxially loaded specimen the SIFs are as follows (Smith, D.J. et al. (2001)):

$$K_{\mathrm{I}} = \sigma\sqrt{\pi a}\,\sin 2\theta,\ K_{\mathrm{II}} = \sigma\sqrt{\pi a}\,\cos\theta\,\sin\theta \tag{24}$$

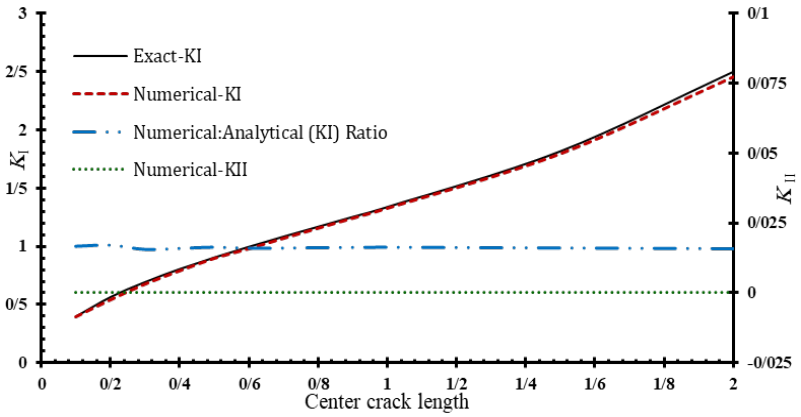

Fig. 11. Adaptation between numerical and theoretical calculation of the SIFs for center crack.

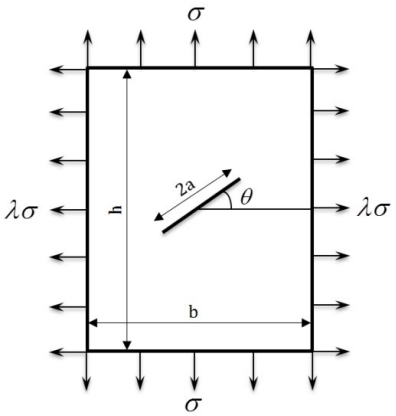

Fig. 12. A single interior inclined crack in a plate subject to biaxial loading.

4.3.1. IGA results for 15, 30, 45 and 60 degrees oriented center cracks

In the following examples, a plate containing $15^\circ, 30^\circ, 45^\circ$ and 60° oriented center cracks are studied and in addition to the visualizing, the stress distributions the values of the stress intensity factors for mixed mode problems are presented. In all cases, the plate is loaded with a uniform far-field traction $\sigma = 1$ applied symmetrically in the vertical direction. Since the uniform tension is considered, so the λ ratio assumed zero. The Young's modulus is taken as $E = 1.0\mathrm{E}+06$ and Poisson's ratio is $\nu = 0.3$. These examples comprise of 4800, 1446, 1912, and 3620 control points and two patches, respectively. Control meshes and parametric spaces are chosen finer around the crack tips. Figure 13, 14, 15, and 16 represent the results of the analysis and the variations of the σ_{xy} on the line consists of the crack surface throughout the domains. In fact, the smooth results lead to have the precise stress distributions, and therefore, the accurate stress intensity factors. In the $15, 30, 45$ and 60 degrees oriented center crack examples the values of the stiff index are 1.0121, 1.1125, 1.1241, and 1.2392, respectively, which indicate the good condition in the stiffness matrices.

In order to calculate the SIFs, we utilized analytical, stress extrapolation, and interaction integral approaches and also compare them with each other. *Table 5* represents the computational results for stress intensity factors which are obtained for four models.

Table 5. Stress intensity factors for oriented center cracks.

Crack Configuration	K_{I} (Analytical)	K_{I} (Stress extrapolation)	K_{II} (Analytical)	K_{II} (Stress extrapolation)	K_{I} (M-integral)	K_{II} (M-integral)
15°	1.1897	1.1867	0.3188	0.3168	1.2690	0.3245
30°	0.9399	0.9395	0.5427	0.5010	1.0196	0.5564
45°	0.5270	0.5267	0.5270	0.5270	0.5486	0.5341
60°	0.4431	0.4461	0.7675	0.7646	0.6029	0.9065

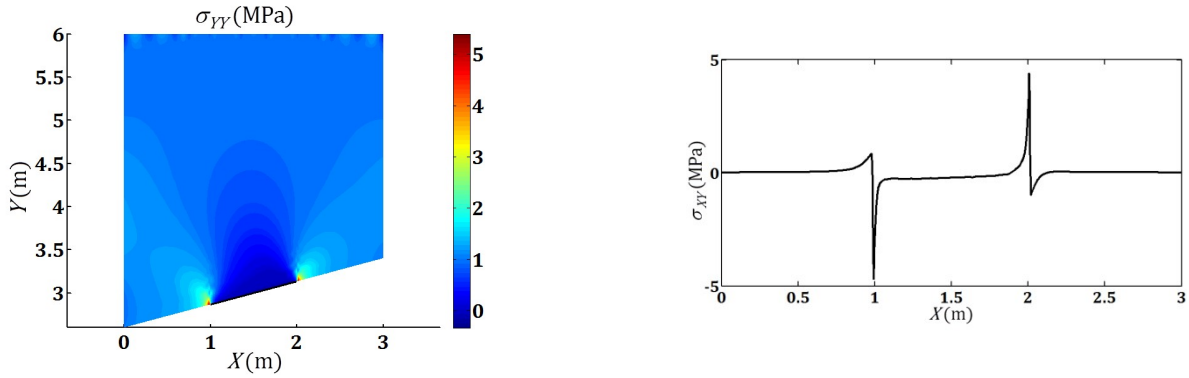

Fig. 13. Representation of the σ_{yy} contour lines and the variations of σ_{xy} in the plate with a 15° CC .

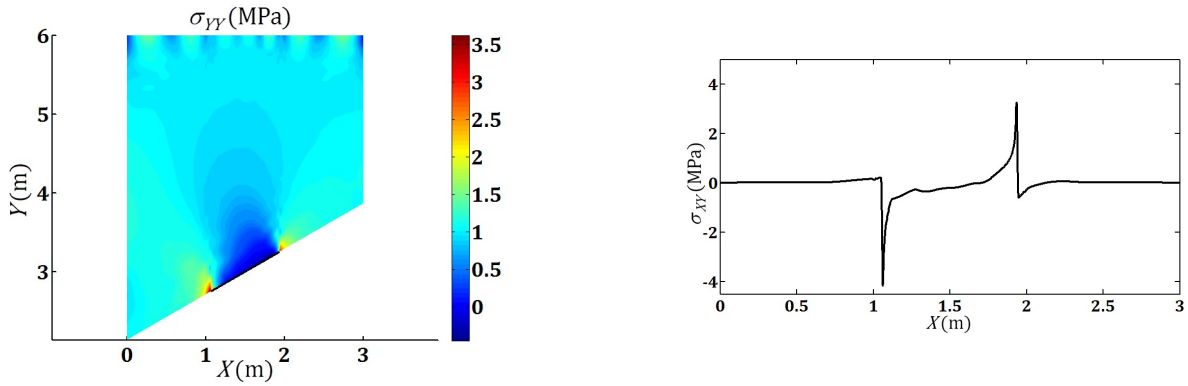

Fig. 14. Representation of the σ_{yy} contour lines and the variations of σ_{xy} in the plate with a 30° CC .

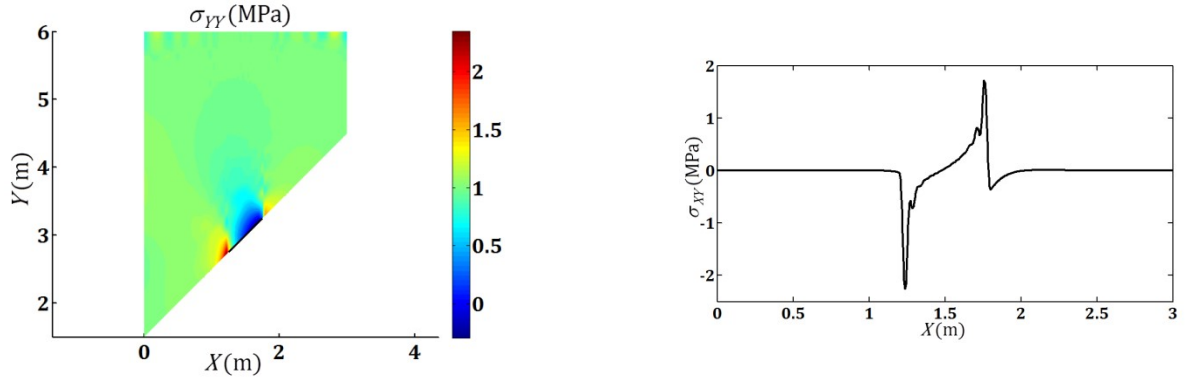

Fig. 15. Representation of the σ_{yy} contour lines and the variations of σ_{xy} in the plate with a 45° CC .

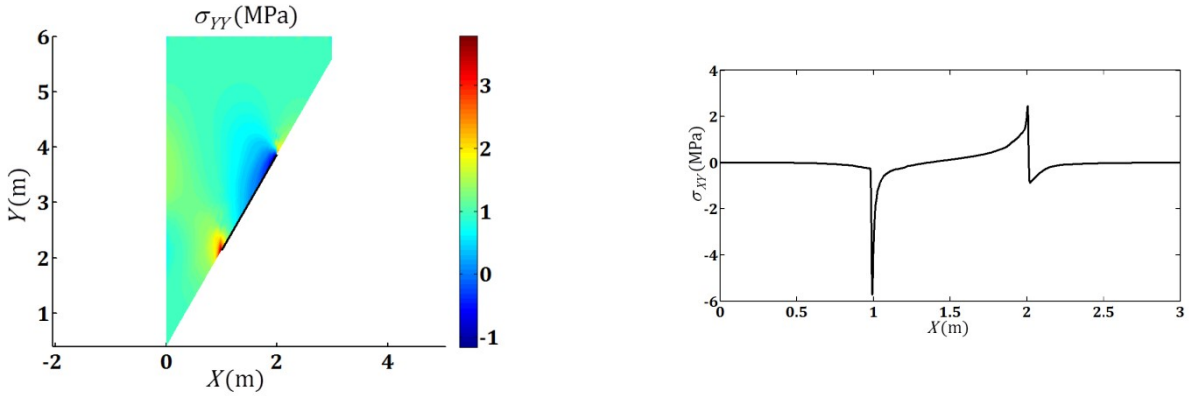

Fig. 16. Representation of the σ_{yy} contour lines and the variations of σ_{xy} in the plate with a 60° CC .

5. Conclusions

The possibility of enhancing a B-spline with knot insertion in the parametric space performed preciously to create cohesive zones and strong discontinuity in the physical space without excessive manipulating of the physical domain. Moreover, the geometries are generated exactly by using NURBS-based isogeometric analysis method. In fact, expressions of well-known *h*, *p*, and *hp* refinement in FEM are implemented in the concept of isogeometric analysis to obtain the best results. The comparisons between analytical-experimental and numerical results for stress intensity factors demonstrate the applicability of the isogeometric analysis method in the context of the fracture mechanics. Moreover, using finer control mesh in the isogeometric analysis method, particularly in the plate with a predefined discontinuity, can achieve a better condition in the stiffness matrix.

Conflict of Interest

The authors declare no conflict of interest.

References

[1] Babuska, I., Melenk, J., The Partition of unity method, *International Journal for Numerical Methods in Engineering*, 40 (1997) 727–758.
[2] Babuška, I., Zhang, Z., The partition of unity method for the elastically supported beam, *Computer Methods in Applied Mechanics and Engineering*, 152(1–2) (1998) 1-18.
[3] Bandyopadhyay, S.N., Deysarker, H.K., Stress intensity factor for a crack emanating from the root of a semi-circular edge notch in a tension plate, *Engineering Fracture Mechanics*, 14(2) (1981) 373-384.
[4] Bazilevs, Y. et al., Isogeometric analysis using T-splines, *Computer Methods in Applied Mechanics and Engineering*, 199(5–8) (2010) 229-263.
[5] Bazilevs, Y., Hsu, M.C., Scott, M.A., Isogeometric fluid–structure interaction analysis with emphasis on non-matching discretizations, and with application to wind turbines, *Computer Methods in Applied Mechanics and Engineering*, 249–252 (2012) 28-41.
[6] Belytschko, T., Black, T., Elastic crack growth in finite elements with minimal remeshing, *International Journal for Numerical Methods in Engineering*, 45(5) (1999) 601-620.
[7] Bhardwaj, G., Singh, I.V., Mishra, B.K., Bui, T.Q., Numerical simulation of functionally graded cracked plates using NURBS based XIGA under different loads and boundary conditions, *Composite Structures*, 126 (2015) 347-359.
[8] Bui, T.Q., Extended isogeometric dynamic and static fracture analysis for cracks in piezoelectric materials using NURBS, *Computer Methods in Applied Mechanics and Engineering*, 295 (2015) 470-509.
[9] Chen, T., Xiao, Z.-G., Zhao, X.-L., Gu, X.-L., A boundary element analysis of fatigue crack growth for welded connections under bending, *Engineering Fracture Mechanics*, 98 (2013) 44-51.
[10] Cottrell, J.A., Hughes, T.J.R., Bazilevs, Y., *Isogeometric Analysis: Toward Integration of CAD and FEA*, Wiley, 2009.
[11] Cottrell, J.A., Hughes, T.J.R., Reali, A., Studies of refinement and continuity in isogeometric structural analysis, *Computer Methods in Applied Mechanics and Engineering*, 196(41–44) (2007) 4160-4183.
[12] Cottrell, J.A., Reali, A., Bazilevs, Y., Hughes, T.J.R., Isogeometric analysis of structural vibrations, *Computer Methods in Applied Mechanics and Engineering*, 195(41–43) (2006) 5257-5296.
[13] COX, M.G., The Numerical Evaluation of B-Splines, *IMA Journal of Applied Mathematics*, 10(2) (1972) 134-149.
[14] Daxini, S.D., Prajapati, J.M., A Review on Recent Contribution of Meshfree Methods to Structure and Fracture Mechanics Applications, *The Scientific World Journal*, 2014 (2014) ID 247172.
[15] de Boor, C., On calculating with B-splines, *Journal of Approximation Theory*, 6(1) (1972) 50-62.
[16] de Klerk, A., Visser, A.G., Groenwold, A.A., Lower and upper bound estimation of isotropic and orthotropic fracture mechanics problems using elements with rotational degrees of freedom, *Communications in Numerical Methods in Engineering*, 24(5) (2008) 335-353.
[17] De Luycker, E., Benson, D.J., Belytschko, T., Bazilevs, Y., Hsu, M.C., X-FEM in isogeometric analysis for linear fracture mechanics, *International Journal for Numerical Methods in Engineering*, 87(6) (2011) 541-565.
[18] Evans, J.A., Bazilevs, Y., Babuška, I., Hughes, T.J.R., n-Widths, sup–infs, and optimality ratios for the k-version of the isogeometric finite element method, *Computer Methods in Applied Mechanics and Engineering*, 198(21–26) (2009) 1726-1741.
[19] Gdoutos, E.E., *Fracture Mechanics: An Introduction*, Springer, 2005.
[20] Ghorashi, S.S., Valizadeh, N., Mohammadi, S., Extended isogeometric analysis for simulation of stationary and propagating cracks, *International Journal for Numerical Methods in Engineering*, 89(9) (2012) 1069-1101.
[21] Gómez, H., Calo, V.M., Bazilevs, Y., Hughes, T.J.R., Isogeometric analysis of the Cahn–Hilliard phase-field model, *Computer Methods in Applied Mechanics and Engineering*, 197(49–50) (2008) 4333-4352.
[22] Hughes, T.J.R., Cottrell, J.A., Bazilevs, Y., Isogeometric analysis: CAD, finite elements, NURBS, exact geometry and mesh refinement, *Computer Methods in Applied Mechanics and Engineering*, 194(39–41) (2005) 4135-4195.
[23] Hughes, T.J.R., Cottrell, J.A., Bazilevs, Y., *Isogeometric Analysis Toward integration of CAD and FEM*, John Wiley & Sons, Inc., 2009.

[24] Joseph, R.P., Purbolaksono, J., Liew, H.L., Ramesh, S., Hamdi, M., Stress intensity factors of a corner crack emanating from a pinhole of a solid cylinder, *Engineering Fracture Mechanics*, 128 (2014) 1-7.
[25] Kim, H.-K., Lee, Y.-H., Decoupling of Generalized Mode I and II Stress Intensity Factors in the Complete Contact Problem of Elastically Dissimilar Materials, *Procedia Materials Science*, 3 (2014) 245-250.
[26] Kim, J.-H., Paulino, G.H., T-stress, mixed-mode stress intensity factors, and crack initiation angles in functionally graded materials: a unified approach using the interaction integral method, *Computer Methods in Applied Mechanics and Engineering*, 192(11–12) (2003) 1463-1494.
[27] Likeb, A., Gubeljak, N., Matvienko, Y., Stress Intensity Factor and Limit Load Solutions for New Pipe-ring Specimen with Axial Cracks, *Procedia Materials Science*, 3 (2014) 1941-1946.
[28] Mohammadi, S., *Extended Finite Element Method: for Fracture Analysis of Structures*, John Wiley & Sons, Inc., 2008.
[29] Oliver, J., Modelling strong discontinuities in solid mechanics via strain softening constitutive equations. Part 2: numerical simulation, *International Journal for Numerical Methods in Engineering*, 39(21) (1996) 3601-3623.
[30] Piegl, L., Tiller, W., *The NURBS Book*, U.S. Government Printing Office, 1997.
[31] Piegl, L.A., Tiller, W., *The Nurbs Book*, Springer-Verlag GmbH, 1997.
[32] Rice, J.R., A Path Independent Integral and the Approximate Analysis of Strain Concentration by Notches and Cracks, *Journal of Applied Mechanics*, 35(2) (1968) 379-386.
[33] Rogers, D.F., *An introduction to NURBS: with historical perspective*, Morgan Kaufmann Publishers, 2001.
[34] Rots, J., Smeared and discrete representations of localized fracture, *International Journal of Fracture*, 51(1) (1991) 45-59.
[35] Schellekens, J.C.J., De Borst, R., On the numerical integration of interface elements, *International Journal for Numerical Methods in Engineering*, 36(1) (1993) 43-66.
[36] Scott, M.A., Li, X., Sederberg, T.W., Hughes, T.J.R., Local refinement of analysis-suitable T-splines, *Computer Methods in Applied Mechanics and Engineering*, 213–216 (2012) 206-222.
[37] Simo, J.C., Oliver, J., Armero, F., An analysis of strong discontinuities induced by strain-softening in rate-independent inelastic solids, *Computational Mechanics*, 12(5) (1993) 277-296.
[38] Smith, D.J., Ayatollahi, M.R., Pavier, M.J., The role of T-stress in brittle fracture for linear elastic materials under mixed-mode loading, *Fatigue and Fracture of Engineering Materials and Structures*, 24(2) (2001) 137-150.
[39] Sutradhar, A., Paulino, G.H., Symmetric Galerkin boundary element computation of T-stress and stress intensity factors for mixed-mode cracks by the interaction integral method, *Engineering Analysis with Boundary Elements*, 28(11) (2004) 1335-1350.
[40] Tur, M., Giner, E., Fuenmayor, F.J., A contour integral method to compute the generalized stress intensity factor in complete contacts under sliding conditions, *Tribology International*, 39(10) (2006) 1074-1083.
[41] Valizadeh, N., Bui, T.Q., Vu, T.V., Minh, H.C., Thai, T., Nguyen, M.N., Isogeometric simulation for buckling, free and forced vibration of orthotropic plates, *International Journal of Applied Mechanics*, 5(2) (2013) 1350017.
[42] Williams, M.L., On the stress distribution at the base of a stationary crack, Journal of Applied Mechanics, 24(1) (1957) 109–114.
[43] Yin, S., Yu, T., Bui, T. Q., Liu, P., Hirose, S., Buckling and vibration extended isogeometric analysis of imperfect graded Reissner-Mindlin plates with internal defects using NURBS and level sets, *Computers & Structures*, 177 (2016) 23-38.
[44] Zhuang, Z., Liu, Z., Cheng, B., Liao, J., *Fundamental Linear Elastic Fracture Mechanics*, In: Zhuang Z, Liu Z, Cheng B, Liao J (eds) Extended Finite Element Method, Academic Press, Oxford, 2014.